
This is an electronic reprint of the original article.
This reprint may differ from the original in pagination and typographic detail.

Author(s): Vähänissi, Ville & Haarahiltunen, Antti & Yli-Koski, Marko & Savin, Hele

Title: Gettering of Iron in Silicon Solar Cells With Implanted Emitters

Year: 2014

Version: Post print

Please cite the original version:

Vähänissi, Ville & Haarahiltunen, Antti & Yli-Koski, Marko & Savin, Hele. 2014. Gettering of Iron in Silicon Solar Cells With Implanted Emitters. IEEE Journal of Photovoltaics. Volume 4, Issue 1. 142-147. ISSN 2156-3381 (printed). DOI: 10.1109/jphotov.2013.2285961.

Rights: © 2014 Institute of Electrical & Electronics Engineers (IEEE). Personal use of this material is permitted. Permission from IEEE must be obtained for all other uses, in any current or future media, including reprinting/republishing this material for advertising or promotional purposes, creating new collective works, for resale or redistribution to servers or lists, or reuse of any copyrighted component of this work in other work.

All material supplied via Aaltodoc is protected by copyright and other intellectual property rights, and duplication or sale of all or part of any of the repository collections is not permitted, except that material may be duplicated by you for your research use or educational purposes in electronic or print form. You must obtain permission for any other use. Electronic or print copies may not be offered, whether for sale or otherwise to anyone who is not an authorised user.

Gettering of Iron in Silicon Solar Cells with Implanted Emitters

Ville Vähänissi, Antti Haarahiltunen, Marko Yli-Koski, and Hele Savin

Aalto University, Department of Micro and Nanosciences, Tietotie 3, 02150 Espoo, Finland

Abstract — We present here experimental results on the gettering of iron in Czochralski-grown silicon by phosphorus implantation. The gettering efficiency and the gettering mechanisms in a high resistivity implanted emitter are determined as a function of both initial iron level and gettering anneal. The results show that gettering in implanted emitters can be efficient if precipitation at the emitter is activated. This requires low gettering temperatures and/or high initial contamination level. The fastest method to getter iron from the bulk is to rapidly nucleate iron precipitates before the gettering anneal. Here this was achieved by a fast ramp to room temperature in between the implantation anneal and the gettering anneal.

Index Terms — gettering, ion implantation, iron, photovoltaic cells, silicon.

I. INTRODUCTION

Ion implantation has been widely used in integrated circuit processing. However, it has not raised much interest in the photovoltaic community until recently. The benefits of implantation, such as better process control and fewer processing steps compared to conventional doping techniques [1, 2, 3], have started to intrigue also the silicon solar cell industry. After all, implantation could provide a great opportunity to reach the ultimate goal: fabrication of low-cost high-efficiency solar cells.

Because of economic reasons, the purity of the silicon feedstock used in photovoltaics is much lower than in integrated circuit industry. [4] Therefore, the high gettering efficiency (GE) [5, 6, 7, 8] provided by the conventional diffused phosphorus emitter is a great benefit in solar cell processing. There are not many studies on the GE obtained by implanted emitters [9] and even fewer where the GEs of diffused and implanted emitters are directly compared. Implanted emitters have typically lower phosphorus concentration, which is likely to decrease the gettering efficiency. However, more interesting is the possible role of the electrically inactive phosphorus [10, 11, 12], which is present after diffusion but not after implantation.

Our goal here is to study the gettering behaviour of iron in silicon by phosphorus implantation with well defined iron concentration levels and varying gettering anneals. In addition to determining the obtainable GE with an implanted emitter, we also study the prevailing mechanisms behind the implantation gettering and compare both the GE and the mechanisms to conventional diffused emitters with higher phosphorus concentration.

II. EXPERIMENTAL

In the experiments p-type silicon wafers with a thickness of 400 μm , a resistivity of 2.7-3.0 Ωcm and a low initial oxygen level (7-9 ppma) were intentionally contaminated to two different iron levels, (i) $1 \times 10^{13} \text{ cm}^{-3}$ (medium) and (ii) $2 \times 10^{14} \text{ cm}^{-3}$ (high). The samples are noted as *medium-Fe* and *high-Fe* later on. The contamination was done by a procedure which is described in more detail in [5]. After contamination a 31 nm thick screen oxide was grown on the wafers at 1000°C to protect the wafers from low energy debris and to reduce implantation induced damage and channelling [13]. Next phosphorus with a dose of $1 \times 10^{15} \text{ cm}^{-2}$ and an energy of 50 keV was implanted on one side of the wafers to form the emitter. Then the screen oxide was removed in diluted hydrofluoric acid solution and the wafers were cleaned in a sequence of SC-1, SC-2 and HF-dip.

After cleaning the wafers were annealed at 1000°C for 30 min to activate the implant and to remove the implantation damage, oxidized at 1000°C for 10 min to passivate the back surface and cooled at the rate of 4 K/min down to the gettering anneal temperature. Four different gettering anneals were used. Gettering anneals A through C followed the implantation anneal directly. In gettering anneal D, the wafers were rapidly cooled down to room temperature, i.e. pulled out from the furnace at 895°C, after the implantation anneal and then loaded again into the furnace at the gettering temperature 620°C. Temperatures and times of the gettering anneals are presented in Table I.

After gettering anneals the backside of the wafers was protected by photoresist. This was followed by the removal of the frontside oxide in buffered HF. Then the sheet resistance of the emitter was measured with four-point probe. The obtained sheet resistance values are presented in Table I.

Interstitial iron concentration in the wafer bulk was measured using the surface photovoltage (SPV) method, which is well-known to measure accurately interstitial iron at low concentrations. The measurement procedure is described in more detail in [5]. In addition, total iron concentration in the phosphorus-doped layer was measured by secondary ion mass spectrometry (SIMS) in selected samples.

Finally, the following supplementary experiments were performed in order to obtain more information about the whereabouts of the gettered iron and the prevailing gettering mechanisms. In the first experiment, some wafers were processed identically to the sample set D but excluding the phosphorus implantation. This means that the samples had no

emitter but they experienced the implantation anneal and gettering anneal D. In the second experiment, from some wafers both the front and back surfaces were removed by etching approximately 23 μm of silicon. The etching was done in a $\text{CH}_3\text{COOH}:\text{HF}:\text{HNO}_3$ solution. Then the wafers were annealed at 1000°C , higher than the applied iron in-diffusion temperature, for 20 min followed by fast cooling. The purpose of the anneal was to dissolve the possible remaining iron in the bulk to the interstitial form. After the dissolution, the interstitial bulk iron concentration was again measured by SPV.

TABLE I
TEMPERATURES AND TIMES OF THE GETTERING ANNEALS AND THE RESULTING SHEET RESISTANCES

Group	Temperature profile	R_s [Ω/\square]
A	2 h at 800°C	96
B	3.5 h at 750°C	94
C	8 h at 620°C	94
D	pullout at 895°C + 8 h at 620°C	85

III. RESULTS

A. Gettering efficiency

Fig. 1 shows a summary of the measured interstitial iron concentration in the bulk after different gettering anneals. At the medium initial iron level (blue columns) the GE is really low with the anneals A and B but a clear improvement is obtained with the anneal C at lower temperature. Intriguingly, anneal D results in remarkably higher GE than the other anneals.

At the high initial iron level (red columns) the GE is high even with the anneal A and strongly increases with lowering gettering temperature (anneals B and C). Already with the anneal B the remaining interstitial iron concentration in the high-Fe wafer is below the level of the medium-Fe wafer and with the anneal C the inversion gets even bigger. With the high initial iron level, the difference between anneal C and anneal D is not as high as with the medium initial level. Nonetheless, also with the high initial iron level, anneal D is the most efficient one and again there is less interstitial iron left than in the similarly treated medium-Fe wafer.

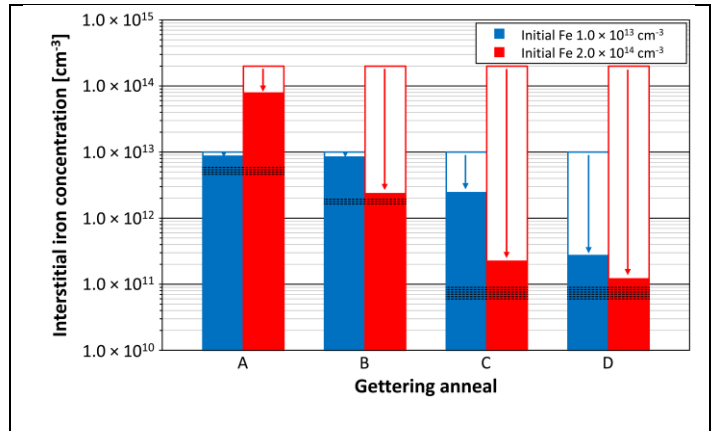


Fig. 1 Measured interstitial iron concentration in the bulk after different gettering anneals. The error estimate of the interstitial iron concentration value is $\pm 2\%$ when iron concentration is below $1 \times 10^{12} \text{ cm}^{-3}$ and $\pm 4\%$ when iron concentration is above $1 \times 10^{12} \text{ cm}^{-3}$. The solid solubility of iron at the gettering anneal temperature [14, 15] is marked with a dotted line.

Fig. 2 presents the minority carrier diffusion length prior to dissociating the Fe_iB_s -pairs in the corresponding samples. Note that the wafers are not standard lifetime references but they still have the emitter present when they are measured by SPV. After anneals A through C the diffusion length behaviour is in agreement with the measured interstitial iron concentration, i.e. the lower the interstitial iron concentration in the bulk, the longer the diffusion length. However, after anneal D, the diffusion length is in contradiction with the interstitial iron concentration. In the high-Fe wafer, the diffusion length is clearly worse after anneal D even though the interstitial iron concentration is lower than after anneal C. With the medium iron level the diffusion length after anneal D is significantly better than after anneal C, but it is not as high as one might expect. The measured interstitial iron concentration after anneal D in medium-Fe wafer is equal to high-Fe wafer after anneal C but the diffusion length is almost a factor of 2 lower.

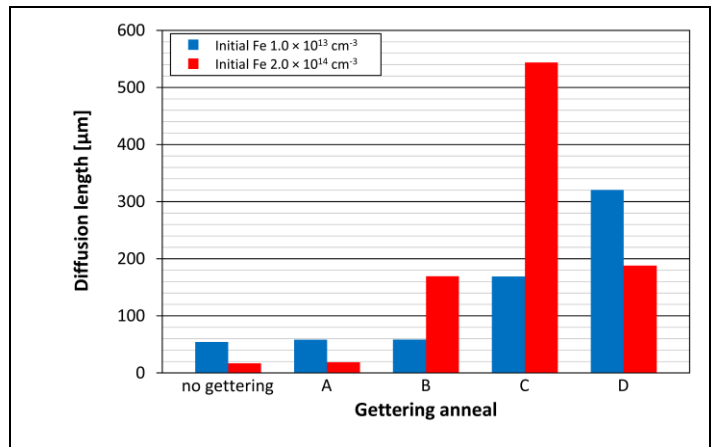
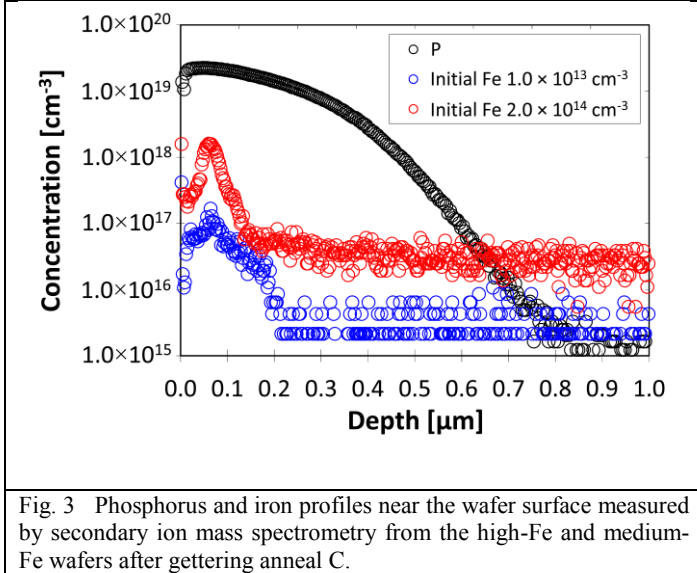


Fig. 2 Measured minority carrier diffusion length prior to dissociating the Fe_iB_s -pairs in the same samples as in Fig. 1.

B. Phosphorus and iron profiles

Phosphorus and iron profiles near the wafer surface measured by SIMS from the high-Fe and medium-Fe wafers after getting anneal C are depicted in Fig. 3. The phosphorus profile is roughly identical in all of our samples since phosphorus diffusion is negligible during the low temperature getting anneals and the ion implantation and the implantation anneal parameters were kept constant. The measured sheet resistance values after the anneals are also in the same range. The peak P concentration is approximately $2 \times 10^{19} \text{ cm}^{-3}$, which is well below the solid solubility value [16] at 1000°C .

SIMS profiles of the iron show that after getting anneal C, iron is not collected only right at the emitter surface but there is a concentration peak that has a maximum approximately at the depth of 60 nm from the wafer surface. A similar iron peak has been reported also by Saga [17] after phosphorus implantation. In that study the peak was attributed to the getting by the end of range defects. In our SIMS profiles, there is a clear difference in the measured iron concentrations between the high-Fe and medium-Fe wafer. The peak iron concentration is a decade larger in the high iron level sample. The amount of gettered iron calculated from the profiles is roughly in agreement with the measured decrease in the interstitial iron concentrations presented in Fig. 1. However, there was some lateral variation observed in the SIMS results in the highly contaminated sample.



IV. DISCUSSION

A. Getting mechanisms

The obtained low GE in the medium-Fe wafers with the anneals A and B could be explained by segregation to the emitter. With the given temperatures and phosphorus

concentration, the segregation coefficient is so low that also the GE due to segregation to the emitter is small. However, with lower temperature (anneal C) a significant improvement is seen, which cannot be explained by pure segregation, indicating the presence of another getting mechanism. The GE seems to have a steep temperature dependence. Similar steep temperature dependence is seen also in the high-Fe wafers. This together with the facts that i) in the high-Fe wafers getting takes place at higher temperatures, ii) getting is faster, and iii) “inversion” occurs, supports the conclusion that the enhanced getting in medium-Fe wafer with anneal C and in high-Fe wafers with anneals A to C takes place due to iron precipitation. It seems that in the medium-Fe wafer the bulk iron reduction rate in anneal C is limited by the iron precipitation rate. In the case of high-Fe wafers the iron reduction rate seems to be limited either by the precipitation rate (anneal A) or the diffusion and segregation of iron to the precipitation sites (anneals B and C). To determine the location of the precipitated iron, more information is needed.

The iron precipitation behaviour with anneal C seems to be directly linked to the iron supersaturation level at the emitter. Most likely iron nuclei are formed at the emitter already during the ramp down from the implant anneal to the getting temperature. Since this is a slow cooling, only a few iron precipitates form, which then grow further in size when the amount of gettered iron increases. Thus, after the getting anneal, there are only a few iron precipitates at the emitter, but they are large in size. The nucleation takes place mainly at the emitter due to the implantation induced damage and segregation. This is supported also by the SIMS results: the amount of gettered iron calculated from the profile matches roughly with the measured decrease in the interstitial iron concentration.

Even though the anneal D is almost identical to the anneal C, the results are quite different. The only difference in processing is the fast cooling to room temperature between the implantation anneal and the getting anneal in the case of D samples. With the medium-Fe wafers the GE is significantly higher in case of anneal D, which implies that the prevailing getting mechanism in anneal D must be precipitation. In anneal D the rapid cool down to room temperature allows iron to nucleate fast creating a higher density of iron precipitates [18] than compared to anneal C. Subsequently, the higher density of iron precipitates results in faster precipitation rate during the following anneal at 620°C . In the best case the precipitation rate, or the getting of iron, can be limited only by diffusion of iron from the bulk. However, it is not clear if the precipitation takes place only at the emitter and thereby further experiments are needed.

B. Role of the electrically inactive phosphorus

Previously, we have made corresponding gettering anneals with diffused emitters. [6] In that study the emitter was formed by in-diffusing phosphorus from a spin-on dopant source for 30 min at 870°C followed by the gettering anneal. Gettering anneals A and B were identical to this study but the temperature of the anneal C was 650°C instead of 620°C used here. The resulting sheet resistance was $\sim 45 \Omega/\text{sq}$. In those experiments the prevailing gettering mechanism was found to be segregation in all anneals (A-C). Now, in Fig. 4 a) we compare the GE of the implanted and diffused emitters after gettering anneals A, B and C, and in Fig. 4 b) the phosphorus profiles of the implanted and diffused emitters measured by SIMS. The gettering efficiency is naturally lower in implanted emitters due to the lower phosphorus concentration. However, this difference cannot be entirely explained by the lower electrically active phosphorus concentration ($\sim 95 \Omega/\text{sq}$ vs. $\sim 45 \Omega/\text{sq}$). We can take into account the phosphorus concentration difference using the segregation coefficient from [6] and the measured phosphorus profile presented in Fig. 3 and Fig. 4 b). After anneals A and B the calculated interstitial iron concentration in the bulk is about $7 \times 10^{12} \text{ cm}^{-3}$ and $2 \times 10^{12} \text{ cm}^{-3}$, respectively. These values are significantly lower than the concentrations measured here as demonstrated also in Fig. 4 a).

One possible reason for the difference in the measured and calculated values is the role of the electrically inactive phosphorus [10, 11, 12]. In [6] the phosphorus layer was made by diffusion and the phosphorus concentration near the emitter surface exceeded the solid solubility value leading to the formation of electrically inactive phosphorus whereas here at the implanted emitter there is no electrically inactive phosphorus present (Fig. 4 b)). This raises the question if the presence of the dead layer is important at least for the segregation based gettering. Another possibility is that the segregation coefficient scales down much faster with decreasing electrically active phosphorus concentration than assumed in [6].

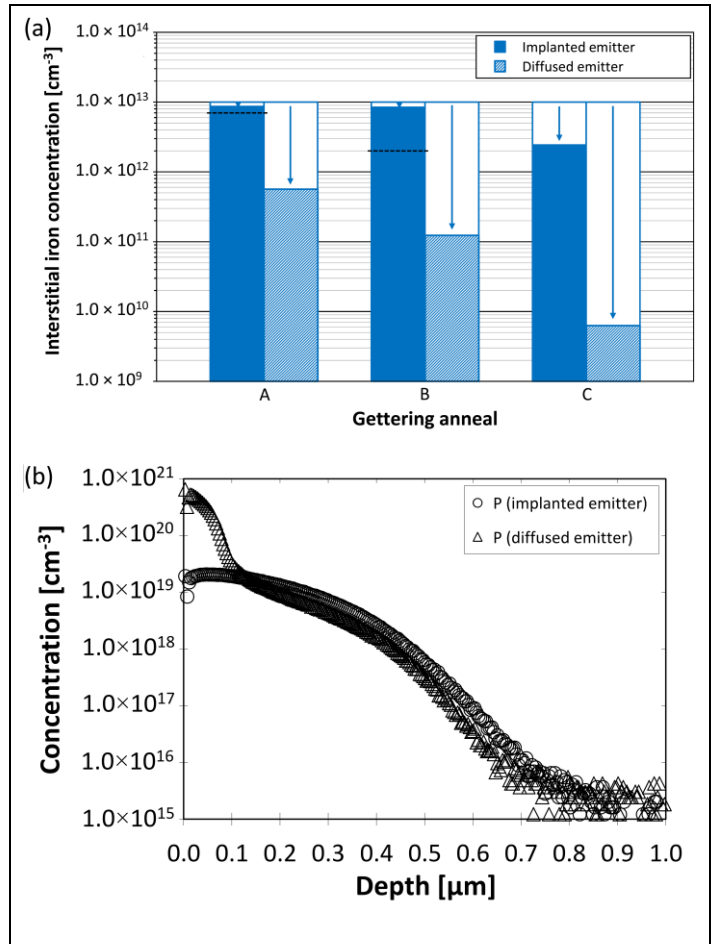


Fig. 4 a) Comparison of interstitial iron concentration in the bulk after gettering with implanted and diffused emitter. The dotted lines show the calculated interstitial iron concentration in the bulk obtained using the segregation coefficient from [6] and the measured phosphorus profile. b) Phosphorus profiles of the implanted and diffused emitters measured by SIMS.

C. Destination of gettered iron

The relatively low minority carrier diffusion length value in high-Fe sample after anneal D was surprising (Fig. 2). It could indicate that not all of the disappeared interstitial iron was actually gettered to the emitter but some of the iron was precipitated either in the wafer bulk and/or on the non-implanted back surface of the wafer due to the above mentioned rapid cooling down to room temperature. In order to verify the hypothesis the supplementary experiments mentioned in the experimental section, i.e. gettering without the presence of an emitter and the combination of surface etching and dissolution anneal, were performed. Fig. 5 presents the interstitial iron concentration in the bulk obtained from these experiments.

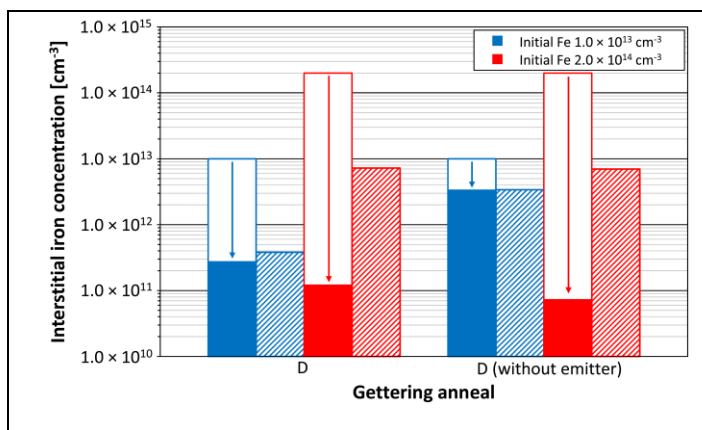


Fig. 5 The interstitial iron concentration in the bulk obtained from the supplementary experiments. Single-colored columns represent the values obtained after getting anneal D in wafers, which have the implanted emitter (left columns) and in wafers with identical thermal anneals but without implantation (right columns). Striped columns represent the values obtained from the same wafers after they have experienced surface etching and dissolution anneal.

We can see from Fig. 5 that the interstitial iron concentration in the medium-Fe sample with the emitter drops approximately a decade lower than without the emitter. This is a clear indication that the iron precipitation rate at the emitter is faster than at the oxide surface, and that segregation and the possible residual damage from the implantation enhance the process. Similar significant difference is seen also in the minority carrier diffusion lengths: 321 μm with the emitter versus 140 μm without the emitter. Thereby, it seems that at the medium contamination level the iron precipitation rate at the emitter is so high that the iron is mostly collected there. Similar strong gettering effect of an implanted layer was observed also in our previous experiments [9], even with a high bulk defect density [19].

In the high-Fe wafers, the results are quite the opposite. The final interstitial iron concentration in the bulk is even a bit smaller without the emitter than with the emitter. This means that high density of iron precipitates, comparable to the density at the emitter, is formed also to the oxide surface in the high-Fe samples. This behavior is clearly different than seen in the medium-Fe samples. The minority carrier diffusion length prior to dissociating the Fe_iB_s -pairs is 188 μm with the emitter and 165 μm without. The most interesting part is that even though the bulk interstitial iron concentration in the high level wafer with an emitter is smaller than in the medium level wafer, the diffusion length is only approximately a half of the value obtained from the medium level wafer. Thus interstitial iron concentration is not limiting the diffusion length in the high-Fe wafer.

The supplementary experiments of surface etching and dissolution provide further information about the location of the gettered iron. In medium-Fe wafers the interstitial iron concentration remains in the same level after surface etching and dissolution (Fig. 5 blue striped columns) confirming that

the gettered iron has not been precipitated in the bulk but has been gettered mainly to the emitter. Again, in the high-Fe wafers, the situation is different. Both with and without an emitter, the bulk interstitial iron concentration increases by approximately two decades as a consequence of the dissolution anneal. Also the diffusion length drops down to the vicinity of 70 μm in both cases. This is a clear indication that in the high-Fe wafers, both with and without the emitter, significant amount of iron ($7 \times 10^{12} \text{ cm}^{-3}$) is precipitated also in the bulk. However, the majority of the gettered iron is still out-diffused and precipitated to the surfaces.

The bulk and surface precipitation in high-Fe samples means that the interstitial iron concentrations or the GE after anneal C and D cannot be directly compared. In addition, in anneal D, it is impossible to make a difference between the precipitation rate to the emitter and to the oxide surface. After both anneal C and anneal D the iron concentration is close to the solubility value (Fig. 1) indicating that the precipitation rate is no longer limiting the gettering process. We obtained a similar concentration of iron remaining in the bulk by simulations (iron precipitation in the bulk and ideal out-diffusion to the surfaces [20]) using a precipitate site density of $5 \times 10^6 \text{ cm}^{-3}$ with a 50 nm fixed capture radius or alternatively using a density of $2 \times 10^7 \text{ cm}^{-3}$ and growing iron precipitates [21]. These values are in a reasonable range with crystal-originated particles (COP), present in modern high quality Czochralski-grown silicon, which are most likely the nucleation sites for iron in the bulk in our study. Our values for precipitate site densities and capture radiuses are in agreement with [22].

D. Impact on solar cell efficiency

One issue is whether the iron precipitation to the bulk in the high iron level case is desirable, like internal gettering in multicrystalline silicon [23], or mostly just a harmful effect. The minority carrier diffusion length in the high-Fe wafer after anneal C is approximately 3 times longer than after anneal D (544 μm vs. 188 μm) even though the bulk interstitial iron concentrations of the wafers are almost the same after gettering. This can be explained by the differences in the gettered iron, especially in the location of iron precipitates. Our results have shown that in anneal C iron precipitation takes place mainly at the emitter while in anneal D some iron precipitates were formed also in the bulk. Thereby after anneal C the minority carrier diffusion length is limited by the interstitial iron concentration whereas after anneal D the limit comes from the iron precipitates in the bulk. The calculated capture coefficient for electrons using the iron precipitate densities of $5 \times 10^6 \text{ cm}^{-3}$ and $2 \times 10^7 \text{ cm}^{-3}$ is in the range of $4\text{-}15 \times 10^{-3} \text{ cm}^3\text{s}^{-1}$. This is roughly ten times higher than the values calculated from the physical surface area and the thermal velocity of the electrons. This apparent discrepancy between physical surface and capture cross section is in agreement with theoretical results [24].

The GE obtained here for an implanted emitter is much lower than for a diffused emitter. [6] However, if the nucleation of iron precipitates takes place, the gettering is robust and the iron concentration should always be reduced to the solubility limit. One drawback is that the iron concentration in the material may not be high enough for reaching sufficient supersaturation for fast precipitation. Another thing to consider is the size of the precipitates at the emitter. By doing the implant anneal and the gettering anneal as separate steps, very fast emitter precipitation can be maintained. Thereby, the gettering process is limited only by the diffusion of iron from the bulk. This allows the size of the precipitates to be kept small, and thus the possible problems related to large iron precipitates, e.g. leakage currents at the emitter, could be avoided. However, it should be kept in mind that eventually the increasing amount of precipitated iron at the emitter starts to limit the operation of the solar cell.

V. CONCLUSIONS

We have experimentally studied the gettering of iron in Czochralski-grown silicon by phosphorus implantation. The prevailing mechanisms behind the implantation gettering, i.e. gettering with a low phosphorus concentration emitter, were found to differ from those present in typical conventional diffused emitters. In addition, the prevailing gettering mechanisms were found to be case sensitive, i.e. the activated mechanisms depend on the initial contamination level and the gettering anneal parameters. In case of high initial iron concentration, gettering takes place mainly through precipitation while in case of lower iron concentration, precipitation becomes dominating only at relatively low temperatures. Iron precipitation takes place mainly at the emitter if iron level is lower than $1 \times 10^{13} \text{ cm}^{-3}$ and the bulk lifetime remains high. If the iron level is high, in the case of a temperature profile that allows iron to form a high density of precipitate nuclei, and thus results in fast gettering, significant amount of iron can precipitate also in the bulk deteriorating the bulk lifetime even in high quality Czochralski-grown silicon. Thus, to reach the best solar cell efficiency, the gettering anneal should be designed to activate the most effective mechanism within the limits of the starting material.

Generally, when the emitter phosphorus concentration is lowered below a certain value (as a result of e.g. implantation), precipitation begins to dominate. In order to reach the best gettering result in this case, the low temperature anneal at the end of the process is crucial annulling the role of a slow cooling. This is opposite to the diffused emitter, in which segregation dominates emphasizing the role of the slow cooling to the actual gettering temperature.

ACKNOWLEDGEMENT

The authors acknowledge the financial support from the Finnish National Technology Agency, Academy of Finland, Okmetic Oyj and Semilab Inc. The corresponding author thanks Walter Ahlström Foundation and the Graduate School in Electronics, Telecommunications and Automation (GETA) for financial support. The authors acknowledge the provision of facilities and technical support by Aalto University at Micronova Nanofabrication Centre.

REFERENCES

- [1] A. Rohatgi, D. Meier, B. McPherson, Y-W. Ok, A. Upadhyaya, J-H. Lai, and F. Zimbardi, "High-throughput ion-implantation for low-cost high-efficiency silicon solar cells", *Energy Procedia*, vol. 15, pp. 10-19, Apr. 2012.
- [2] M. Sheoran, M. Emsley, M. Yuan, D. Ramappa, and P. Sullivan, "Ion-implant doped large-area n-type Czochralski high-efficiency industrial solar cells", in *Proc. 38th IEEE Photovoltaic Spec. Conf. Rec.*, Jun. 2012, pp. 2254-2257.
- [3] V. Prajapati, T. Janssens, J. John, J. Poortmans, and R. Mertens, "Diffusion-free high efficiency silicon solar cells", *Prog. Photovoltaics: Res. Appl.*, vol. 21, no. 5, pp. 980-985, Aug. 2013.
- [4] A. Müller, M. Ghosh, R. Sonnenschein, and P. Woditsch, "Silicon for photovoltaic applications", *Mater. Sci. Eng. B*, vol. 134, no. 2-3, pp. 257-262, Oct. 2006.
- [5] V. Vähänissi, A. Haarahiltunen, H. Talvitie, M. Yli-Koski, and H. Savin, "Impact of phosphorus gettering parameters and initial iron level on silicon solar cell properties", *Prog. Photovoltaics: Res. Appl.*, vol. 21, no. 5, pp. 1127-1135, Aug. 2013.
- [6] H. Talvitie, V. Vähänissi, A. Haarahiltunen, M. Yli-Koski, and H. Savin, "Phosphorus and boron diffusion gettering of iron in monocrystalline silicon", *J. Appl. Phys.*, vol. 109, no. 9, pp. 093505-1-093505-5, May 2011.
- [7] S. P. Phang, and D. Macdonald, "Direct comparison of boron, phosphorus, and aluminum gettering of iron in crystalline silicon", *J. Appl. Phys.*, vol. 109, no. 7, pp. 073521-1-073521-6, Apr. 2011.
- [8] P. Manshanden, and L.J. Geerligs, "Improved phosphorous gettering of multi-crystalline silicon", *Sol. Energy Mater. Sol. Cells*, vol. 90, no. 7-8, pp. 998-1012, May 2006.
- [9] A. Haarahiltunen, H. Talvitie, H. Savin, O. Anttila, M. Yli-Koski, M. I. Asghar, and J. Sinkkonen, "Gettering of iron in silicon by boron implantation", *J. Mater. Sci. – Mater. Electron.*, vol. 19, no. 1 (suppl.), pp. 41-45, Dec. 2008.
- [10] V. Vähänissi, A. Haarahiltunen, H. Talvitie, M. I. Asghar, M. Yli-Koski, and H. Savin, "Effect of oxygen in low temperature boron and phosphorus diffusion gettering of iron in Czochralski-grown silicon", *Solid State Phenomena*, vol. 156-158, pp. 395-400, Oct. 2010.
- [11] B. Tryznadlowski, A. Yazdani, R. Chen, and S. T. Dunham, "Coupled modeling of evolution of impurity/defect distribution and cell performance", in *Proc. 38th IEEE Photovoltaic Spec. Conf. Rec.*, Jun. 2012, pp. 217-220.
- [12] A. Cuevas, D. Macdonald, M. Kerr, C. Samundsett, A. Sloan, S. Shea, A. Leo, M. Mrcarica, and S. Winderbaum, "Evidence of impurity gettering by industrial phosphorus diffusion", *Proc. 28th IEEE Photovoltaic Spec. Conf. Rec.*, Sep. 2000, pp. 244-247.

- [13] S. Wolf, and R. N. Tauber, "Ion implantation for VLSI", in *Silicon Processing for the VLSI Era Volume 1 – Process Technology*, California, Lattice Press, 1987, pp. 323-325.
- [14] M. Aoki, A. Hara, and A. Ohsawa, "Fundamental properties of intrinsic gettering of iron in a silicon wafer", *J. Appl. Phys.*, vol. 72, no. 3, pp. 895-898, Aug. 1992.
- [15] J. D. Murphy, and R. J. Falster, "Contamination of silicon by iron at temperatures below 800°C", *Phys. Status Solidi – Rapid Res. Lett.*, vol. 5, no. 10-11, pp. 370-372, Nov. 2011.
- [16] V. E. Borisenko, and S. G. Yudin, "Steady-state solubility of substitutional impurities in silicon", *Phys. Status Solidi A*, vol. 101, no. 1, pp. 123-127, May 1987.
- [17] K. Saga, "Gettering behavior of transition metals in low energy, high dose ion implanted silicon", *Solid State Phenomena*, vol. 187, pp. 283-286, Apr. 2012.
- [18] A. Haarahiltunen, M. Yli-Koski, and H. Savin, "Effect of thermal history on iron precipitation in crystalline silicon", *Energy Procedia*, vol. 8, pp. 355-359, Apr. 2011.
- [19] H. Talvitie, M. Yli-Koski, A. Haarahiltunen, V. Vähänissi, M. I. Asghar, and H. Savin, "Experimental study of iron redistribution between bulk defects and boron doped layers in silicon wafers", *Phys. Status Solidi A*, vol. 208, no. 10, pp. 2430-2436, Oct. 2011.
- [20] H. Hieslmair, S. Balasubramanian, A. A. Istratov, and E. R. Weber, "Gettering simulator: physical basis and algorithm", *Semicond. Sci. Technol.*, vol. 16, no. 7, pp. 567-574, Jul. 2001.
- [21] H. Hieslmair, A. A. Istratov, T. Heiser, and E. R. Weber, "Evaluation of precipitate densities and capture radii from the analysis of precipitation kinetics", *J. Appl. Phys.*, vol. 84, no. 2, pp. 713-717, Jul. 1998.
- [22] J. Murphy, and R. Falster, "The relaxation behaviour of supersaturated iron in single-crystal silicon at 500 to 750°C", *J. Appl. Phys.*, vol. 112, no. 11, pp. 113506-1-113506-7, Dec. 2012.
- [23] R. Krain, S. Herlufsen, and J. Schmidt, "Internal gettering of iron in multicrystalline silicon at low temperature", *Appl. Phys. Lett.*, vol. 93, no. 15, pp. 152108-1-152108-3, Oct. 2008.
- [24] P. S. Plekhanov, and T. Y. Tan, "Schottky effect model of electrical activity of metallic precipitates in silicon", *Appl. Phys. Lett.*, vol. 76, no. 25, pp. 3777-3779, Jun. 2000.

- [1] A. Rohatgi, D. Meier, B. McPherson, Y-W. Ok, A. Upadhyaya, J-H. Lai, and F. Zimbardi, "High-throughput ion-implantation for low-cost high-efficiency silicon solar cells", *Energy Procedia*, vol. 15, pp. 10-19, 2012.
- [2] M. Sheoran, M. Emsley, M. Yuan, D. Ramappa, and P. Sullivan, "Ion-implant doped large-area n-type Czochralski high-efficiency industrial solar cells", in: Proceedings of the 38th IEEE Photovoltaic Specialists Conference (PVSC), Austin, Texas, 2012.
- [3] V. Prajapati, T. Janssens, J. John, J. Poortmans, and R. Mertens, "Diffusion-free high efficiency silicon solar cells", *Progress in Photovoltaics: Research and Applications*, in press, DOI: 10.1002/pip.2189, 2012.
- [4] A. Müller, M. Ghosh, R. Sonnenschein, and P. Woditsch, "Silicon for photovoltaic applications", *Materials Science and Engineering B*, vol. 134, pp. 257-262, 2006.
- [5] V. Vähänissi, A. Haarahiltunen, H. Talvitie, M. Yli-Koski, and H. Savin, "Impact of phosphorus gettering parameters and initial iron level on silicon solar cell properties", *Progress in Photovoltaics: Research and Applications*, in press, DOI: 10.1002/pip.2215.
- [6] H. Talvitie, V. Vähänissi, A. Haarahiltunen, M. Yli-Koski, and H. Savin, "Phosphorus and boron diffusion gettering of iron in monocrystalline silicon", *Journal of Applied Physics*, vol. 109, 093505, 2011.
- [7] S. P. Phang, and D. Macdonald, "Direct comparison of boron, phosphorus, and aluminum gettering of iron in crystalline silicon", *Journal of Applied Physics*, vol. 109, 073521, 2011.
- [8] P. Manshanden, and L.J. Geerligs, "Improved phosphorous gettering of multi-crystalline silicon", *Solar Energy Materials and Solar Cells*, vol. 90, pp. 998-1012, 2006.
- [9] A. Haarahiltunen, H. Talvitie, H. Savin, O. Anttila, M. Yli-Koski, M. I. Asghar, and J. Sinkkonen, "Gettering of iron in silicon by boron implantation", *Journal of Materials Science: Materials in Electronics*, vol. 19, pp. S41-S45, 2008.
- [10] V. Vähänissi, A. Haarahiltunen, H. Talvitie, M. I. Asghar, M. Yli-Koski, and H. Savin, "Effect of oxygen in low temperature boron and phosphorus diffusion gettering of iron in Czochralski-grown silicon", *Solid State Phenomena*, vol. 156-158, pp. 395-400, 2010.
- [11] B. Tryznadlowski, A. Yazdani, R. Chen, and S. T. Dunham, "Coupled modeling of evolution of impurity/defect distribution and cell performance", in: Proceedings of the 38th IEEE Photovoltaic Specialists Conference (PVSC), Austin, Texas, 2012.
- [12] A. Cuevas, D. Macdonald, M. Kerr, C. Samundsett, A. Sloan, S. Shea, A. Leo, M. Mrcarica, and S. Winderbaum, Conference Record of the 28th IEEE Photovoltaic Specialists Conference, 2000 (unpublished) , pp. 244-247.
- [13] S. Wolf, and R. N. Tauber, "Ion implantation for VLSI", in *Silicon Processing for the VLSI Era Volume 1 – Process Technology*, California, Lattice Press, 1987, pp. 323-325.
- [14] M. Aoki, A. Hara, and A. Ohsawa, "Fundamental properties of intrinsic gettering of iron in a silicon wafer", *Journal of Applied Physics*, vol. 72, pp. 895-898, 1992.
- [15] J. D. Murphy, and R. J. Falster, "Contamination of silicon by iron at temperatures below 800°C", *Physica Status Solidi – Rapid Research Letters*, vol. 5, pp. 370-372, 2011.
- [16] V. E. Borisenko, and S. G. Yudin, "Steady-state solubility of substitutional impurities in silicon", *Physica Status Solidi A*, vol. 101, pp. 123-127, 1987.
- [17] K. Saga, "Gettering behavior of transition metals in low energy, high dose ion implanted silicon", *Solid State Phenomena*, vol. 187, pp. 283-286, 2012.
- [18] A. Haarahiltunen, M. Yli-Koski, and H. Savin, "Effect of thermal history on iron precipitation in crystalline silicon", *Energy Procedia*, vol. 8, pp. 355-359, 2011.
- [19] H. Talvitie, M. Yli-Koski, A. Haarahiltunen, V. Vähänissi, M. I. Asghar, and H. Savin, "Experimental study of iron redistribution between bulk defects and boron doped layers in silicon wafers", *Physica Status Solidi A*, vol. 208, pp. 2430-2436, 2011.
- [20] H. Hieslmair, S. Balasubramanian, A. A. Istratov, and E. R. Weber, "Gettering simulator: physical basis and algorithm", *Semiconductor Science and Technology*, vol. 16, pp. 567-574, 2001.
- [21] H. Hieslmair, A. A. Istratov, T. Heiser, and E. R. Weber, "Evaluation of precipitate densities and capture radii from the analysis of precipitation kinetics", *Journal of Applied Physics*, vol. 84, pp. 713-717, 1998.
- [22] J. Murphy, and R. Falster, "The relaxation behaviour of supersaturated iron in single-crystal silicon at 500 to 750°C", *Journal of Applied Physics*, vol. 112, 113506, 2012.
- [23] R. Krain, S. Herlufsen, and J. Schmidt, "Internal gettering of iron in multicrystalline silicon at low temperature", *Applied Physics Letters*, vol. 93, 152108, 2008.
- [24] P. S. Plekhanov, and T. Y. Tan, "Schottky effect model of electrical activity of metallic precipitates in silicon", *Applied Physics Letters*, vol. 76, pp. 3777-3779, 2000.